IV. Source rocks and basin modeling

1. Introduction

The study area is located in the South Celtic Sea and in the St's George basins. A Basin Analysis was performed in order to build reliable model of the petroleum system with emphasis in the source rocks, a characterization of the petroleum potential was done in two plays. A total of nine 1D models of drilled wells and 14 model of pseudo wells were done to determinate the potential hydrocarbon generation and the maturity of the source rock. Also, 2D cross section models in the traps sector were built. This study is important in order to reconstruct the history of the sedimentary basin, which will affect the prediction of the generation, expulsion, migration and preservation of the hydrocarbon.

2. Data set/Methodology

The data set consisted of geochemical reports from 12 exploration wells (Table 4.1), as well as lithological, well log and mud reports. Regarding to the methodology and workflow, first a compilation of different data was done, for example different excel files were built from well reports, such as pressure (mud weight), Borehole Temperature data and geochemical data, among other parameters. After these, the calibration of nine drilled wells against well data was done. The calibrated data was used to build the models for 14 pseudo wells, which were located in the kitchen sector and near the trap. 2D models were carried out in both prospect sectors. In order to characterize the source rock, regional TOC maps were built. In all the steps a literature review was done. The final step was the analysis and conclusion of the results.

Table 4.1: Data set used in this project.

Well	Well class	Basin	TOC	S1	S2	HI	OI	PI	Tmax	Vitrinite Reflectane
93_02_3	0.05% background gas	South Celtic Sea	46	–	–	46	–	–	–	9
93_02_1	Dry	South Celtic Sea	45	–	–	16	–	16	16	28
102_29_1	Dry	South Celtic Sea	30	–	–	–	–	–	–	16
106_24_1	Dry	South Celtic Sea	32	–	–	–	–	–	–	
103_01_1	Dragon field (sub economic)	St George's Channel	48	29	29	29	–	28	28	14
106_28_1	Dry	St George's Channel	91	10	7	29	29	18	29	16
106_24a-2b	Dry	St George's Channel	–	–	–	–	–	–	–	4
106_18_1	Dry	St George's Channel	36	12	12	12	–	–	12	5
103_2_1	Dry	St George's Channel	–	–	–	–	–	–		5
107_21_1	Dry	St George's Channel	230	58	54	54	60	–	54	34
107_16_1	Dry	St George's Channel	98	–	–	–	–	–	79	14
Σ			656	109	102	186	89	62	218	145

3. Background information

The interval of the Early Jurassic came after the end of the Triassic mass extinction and global warming event, moreover, the break-up of the Pangea and continental rifting occurred in the Early Jurassic which formed marine and continental rift basins with yield into source rocks generation (Fleet *et al*., 1987). The source rocks are related to marine infiltrations, such as the intrusion of the Tethyan Ocean and the opening of the central Atlantic. The direction of the marine inversion of the Tethyan was to the NW. The deposition of the Early Jurassic was marked by an initial negative carbon isotope excursion (-2%$_{0,}$ Ruhl *et al*., 2016). Meanwhile, by the Late Pliensbachian a positive excursion (+2%$_0$ of Ruhl *et al*., 2016) happened. There were two major erosions event, one happened in the Berriasian (McMahon & Turner, 1998) and is commonly called BCU (or called by Hilils in1988, as the ‘Cimmerian Unconformity’), which is a widespread unconformity which is best developed in the basin margins but becomes paraconfomable in the depocenters. Another exhumation occurs in the Late Cretaceous-Paleocene (BTU) followed by a basin inversion in the Oligo-Miocene (Rowell, 1995).

4. Results

4.1 Calibration of wells

A total of nine 1D models of drilled wells were calibrated. The well 106_18_1 is one of the wells that has more data to calibrate. Fig. 4.1 shows the depth plot against the calibration data.

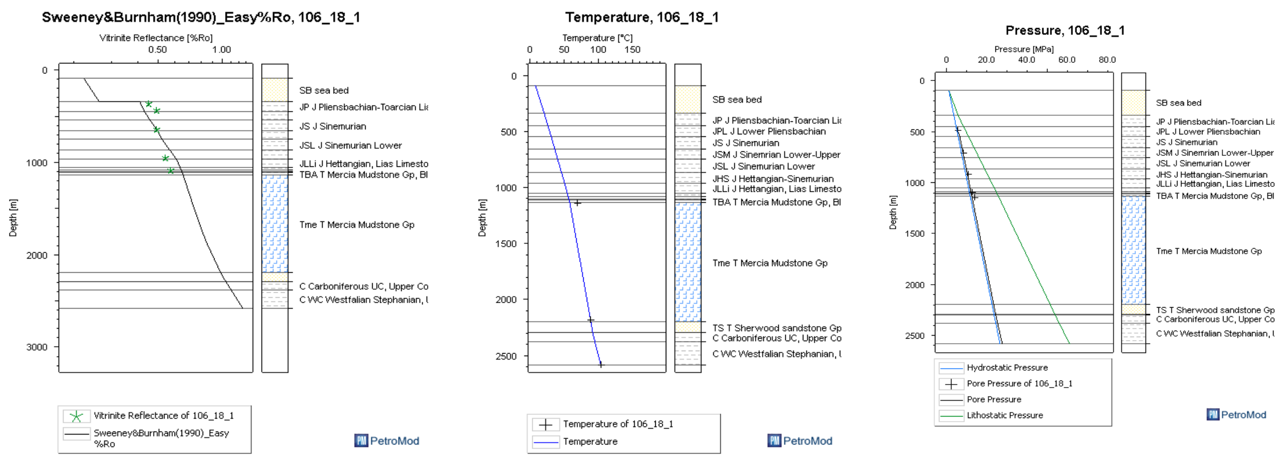

Figure 4.1: Depth plots against calibration data, well 106_18_1.

According to Corry *et al*., (1998), the present-day heat flow for the Celtic Sea basins goes from 59 to 81 mWm^{-2}, the high values are related to large thickness of sediments, this range was used for the present heat flow calibration. The calibration of the past heat flow was done considering the rifting stages that affected the Celtic Sea Basins (to see the others well calibrated, Appendix 1.6).

4.2 Source rock characterization

4.2.1 Well Source rock characterization

Well 106_28_1 (Fig. 4.2)

Maturity: The Lower Oligocene, Eocene and Lower Jurassic are immature, but there is an increase in the value of Ro from 0.2 (Lower Oligocene) to almost 0.5 (Lower Jurassic).

Richness: The Middle Jurassic has a fair richness with an average of 0.83% (TOC average calculations per well in Appendix 1.1). The Lower Jurassic (arithmetic average of 1.30%) has a good TOC content for the Pliensbachian and the Sinemurian rocks with 1.34% and 1.95%, respectively. Meanwhile, all the samples of the Upper Triassic are fair (0.31% average).

Quality: The quality of the Lower Jurassic is fair (J Lower Toarcian) to good (J Pliensbachian and J Late Sinemurian).

Type of kerogen: The type of kerogen in the Middle Jurassic is a mixture of type III and VI. Meanwhile, in the Lower Jurassic is a mixture between type II, II-III and III (J Pliensbachian, J Sinemurian). The Upper Triassic shows a kerogen type III.

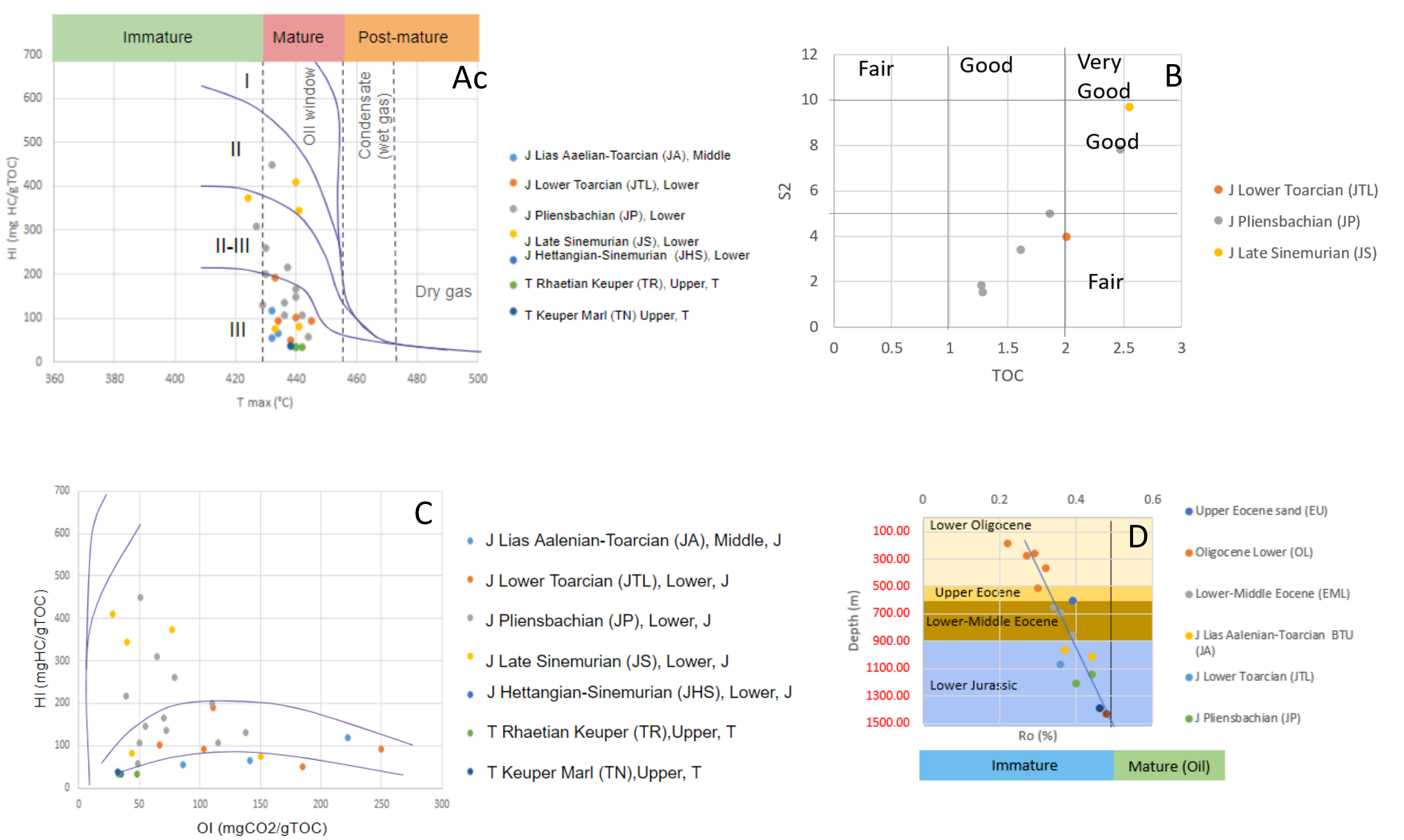

Figure 4.2: A: Plot HI vs Tmax; B: Plot S2 (mg/g rock); C: Plot HI vs OI; D: Plot Depth vs Ro.

4.2.2 Regional Source rock characterization

Table 4.2 shows the 656 TOC geochemical data that were collected, most of the samples are from the Jurassic, only 4, 6 and 3 samples are from the Paleogene, Lower Cretaceous and Carboniferous, respectively. The heterogeneity of a sample population is shown with the coefficient of variation (Homogenous<0.5; heterogeneous between 0.5-1; very heterogeneous>1).

The average and median values of TOC for the Carboniferous, Upper Triassic and Lower Cretaceous, are of a fair source rock. The Paleogene samples have a richness of a very good source rock (8.9%) and the median value corresponds to a good source rock, these values are related to samples of coals with very high TOC in the well 106_24_1. The standard deviation and the coefficient of variation for the Carboniferous, Upper Triassic, Lower Cretaceous and Paleogene indicates a heterogeneous population.

Table 4.2: Number of samples of TOC for the different Epoch and the statistical parameters.

Period	N° samples	Arithmetic Average (%)	Median (%)	Standard deviation	Coefficient variation
Paleogene (Eocene)	4	8.9	1.06	16.16	1.8
Lower Cretaceous	6	0.54	0.4	0.42	0.78
Upper Jurassic	142	3.15	0.7	7.79	2.47
Middle Jurassic	310	1.25	0.85	4.31	3.44
Lower Jurassic	126	1.20	0.92	0.948	0.78
Upper Triassic	65	0.24	0.125	0.28	1.16
Carboniferous	3	0.37	0.38	0.205	0.554

The greater arithmetic average and mean values correspond to the Jurassic period which in all of the Epoch is higher than 1%, indicating a good source rock. The Lower Jurassic (126 samples) has an average of 1.20% and has the highest median value is 0.92%, indicating a fair to good source rock; the standard deviation and the coefficient of variation indicates a homogenous population.

The Middle Jurassic (310 samples) has an average of 1.25% and a median value of 0.85%. The Upper Jurassic (142 samples) has the greater arithmetic average with 3.15% and a median value of 0.7% (fair source rock), the high average is caused by coal and coaly shaly samples with TOC >11% that are in the north part of the basin (wells 107_21_1 and 107_16_1, see Appendix 1.1). The St. Dv. and the coefficient of variation for the Upper and Middle Jurassic indicate a heterogeneous population.

The Hydrogen Index and Oxygen Index graph (Fig. 4.3A) shows for the Lower Jurassic (data available for the well 106_28_1) a scattered data from some samples in the II, III and IV type of kerogen (HI values up to 450 mg/g). For the Middle Jurassic the data is scattered with a high proportion of samples in the kerogen type III zone and for the Upper Jurassic (data available only for the well 107_21_1) the type of kerogen is IV (between 45 and 270 mg/g OI and 30-120 mg/g HI).

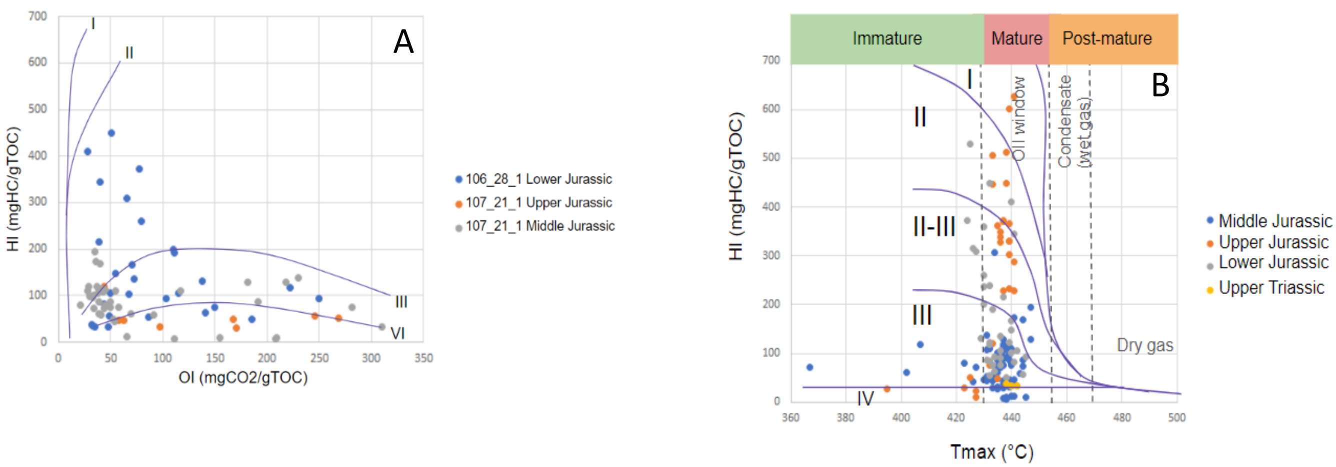

Figure 4.3: A: Plot HI vs OI; B: Plot HI vs Tmax

The Hydrogen Index and Tmax graph (Fig. 4.3B) shows for the Lower Jurassic a kerogen type II, II-III and III. Meanwhile, for the Middle Jurassic a kerogen type III and II-II and for Upper Jurassic there is a big scattering of values from Type IV until type I.

The Fig. 4.4 shows the sampe plot as the Fig. 4.3B but in this case the samples are differentiated by different TOC zones. The samples with a high TOC (2-3%) correspond to the kerogen type I, II and II-III, most of these samples are from the Upper and Lower Jurassic, meanwhile the good source rock is from the Jurassic (1-2%) and correponds mostly to kerogen type III.

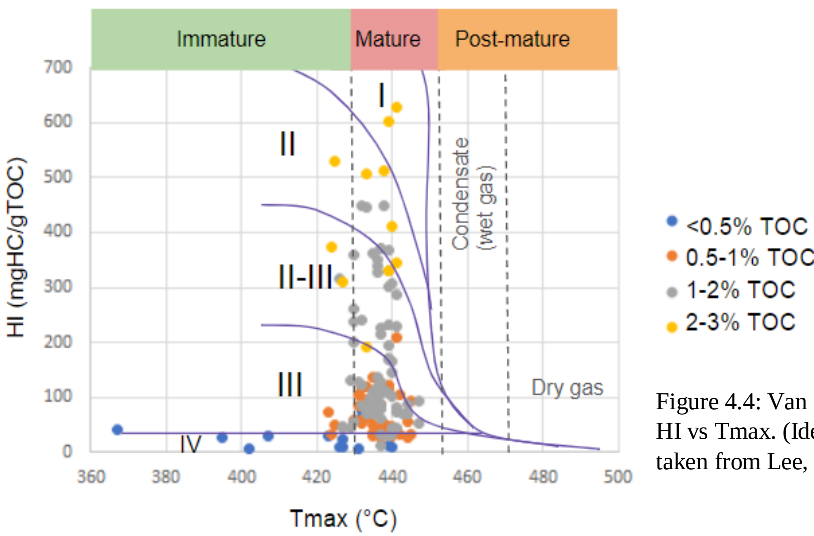

Figure 4.4: Van Krevelen diagram, HI vs Tmax. (Idea of the graph taken from Lee, J, 2017)

As a conclusion, the richest source rock is found in the Jurassic interval, being the Lower Jurassic the most important one with higher mean value and a homogenous population. For the SCSB, the Sinemurian is the interval with higher TOC content with 2.47% followed by the Pliensbachian with 1.58 % and the Hettangian with an average of 1.5% (Table 4.3). On the other hand, in the SGCB the Pliensbachian interval is the one with higher TOC content (1.49%) followed by the Sinemurian with 1.24 % and the Hettangian in this basin is a fair source with 0.8%, therefore, it's not considered as a potential source in this basin. Moreover, the deposition of the Early Jurassic was marked by an initial negative carbon isotope excursion, this positive carbon isotope excursion is related to higher productivity of organic carbon and is a geochemical index for generation of source rocks.

The Fig. 4.5 shows the two regional TOC maps for the Lower Jurassic, (to see others maps such as TOC only for Hettangian, Sinemuriand and Pliensbachian see Appendix 1.4). One TOC map was built using geochemical (Fig. 4.5B) data and the other was built using the geochemical data and the TOC calculated using well log data (Fig. 4.5A), Resistivity and Sonic (to see logR and the baseline see Appendix 1.3). Both maps have the same trend, where it can be seen that the SCSB is the basin with highest TOC content.

Table 4.3: TOC content per basin and well at different geological Ages. Obs: TOC data from 106_20_1; 106_28_2; 93_02_2 and 102_28_02; 103_1_1 (JP) calculated from well log data (Appendix1.3).

TOC content (%) JH		
93_2_2	1.9	Average TOC SCSB: 1.5 %
102_29_1	1.1	
106_28_1	1	Average TOC SGCB: 0.8 %
106_18_1	0.81	
106_20_1	0.5	

TOC content (%) JS		
93_2_2	1.9	Average TOC SCSB: 2.47 %
102_29_1	3.04	
106_20_1	1	Average TOC SGCB: 1.24 %
106_28_1	1.94	
106_18_1	0.8	

TOC content (%) JP		
102_28_2	1.2	Average TOC SCSB: 1.58%
93_2_3	1.67	
102_29_1	1.89	
103_1_1	1.6	Average TOC SGCB: 1.49 %
106_20_1	1.26	
106_28_1	1.36	
106_18_1	1.748	

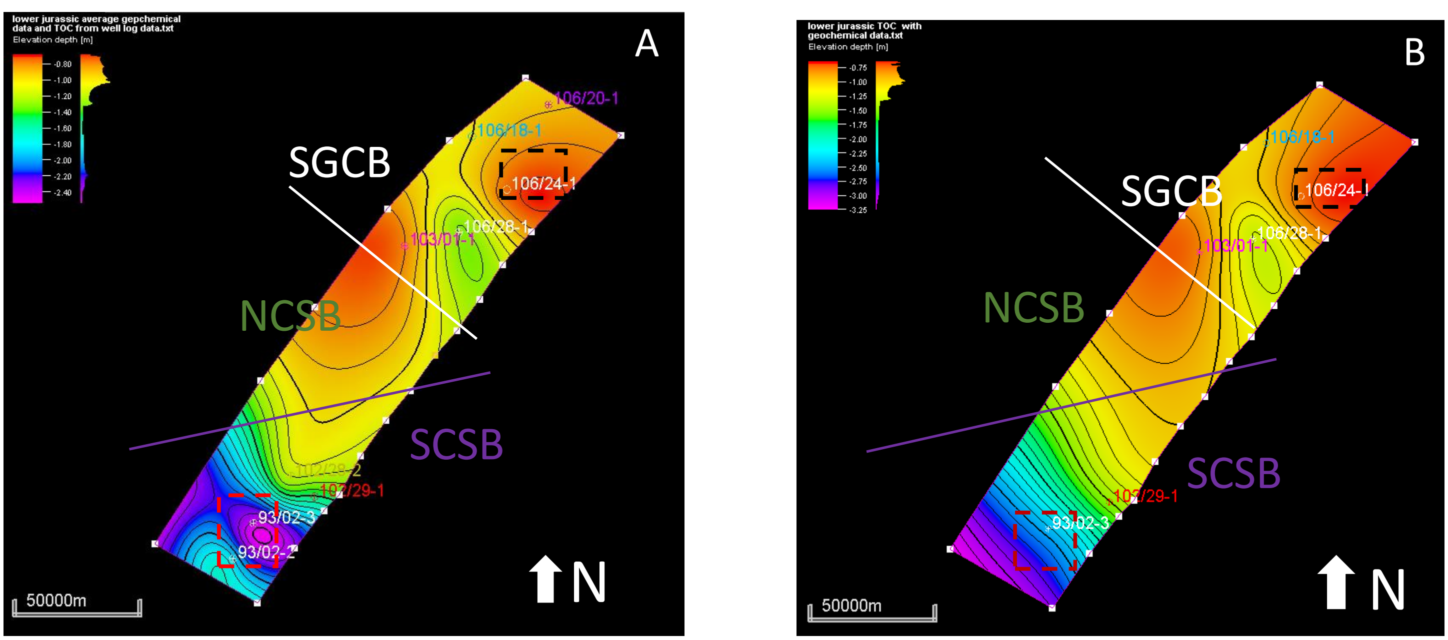

Figure 4.5: A: Regional TOC map using geochemical and TOC calculated from well log data; B: Regional TOC map only with geochemical data (well that were used for build the map are shown). Red square: location of the Fig. 4.7B. Black square: location of the Fig. 4.7A.

The Fig. 4.6A shows the depth model with the gamma ray for the SCSB (given by the seismic interpreter), the highest value corresponds to the Pliensbachian interval. The Fig. 4.6B shows the depth model with TOC values for the Pliensbachian to Triassic interval, using only TOC from geochemical data. It can be seen a good correlation, where the highest TOC interval has the highest gamma ray.

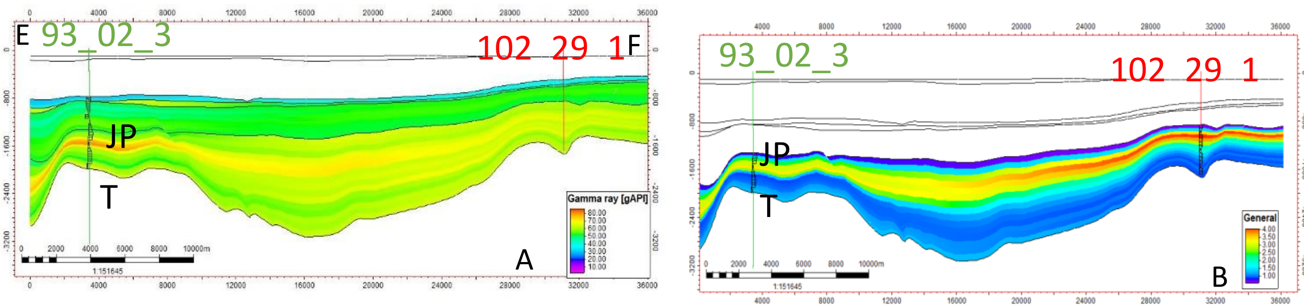

Figure 4.6: A: Gamma ray for the cross section EF (Fig. 4.5A); B: Depth model with TOC value (cross section EF).

The Fig. 4.7B, shows the thickness of the Triassic to the Pliensbachian source rocks in the SCSB (location in Fig. 4.6A), which has a thickness from 250 m to greater than 2,000 m. The thickest interval is located in in the NW depocenters which are limited by NE-SW faults. For the SGCB (location in Fig. 4.6A), the thickness from the Sinemurian to the Pliensbachian interval goes from 100 m to 1,000 m (Fig. 4.7B). The thickest interval is in the NW sector.

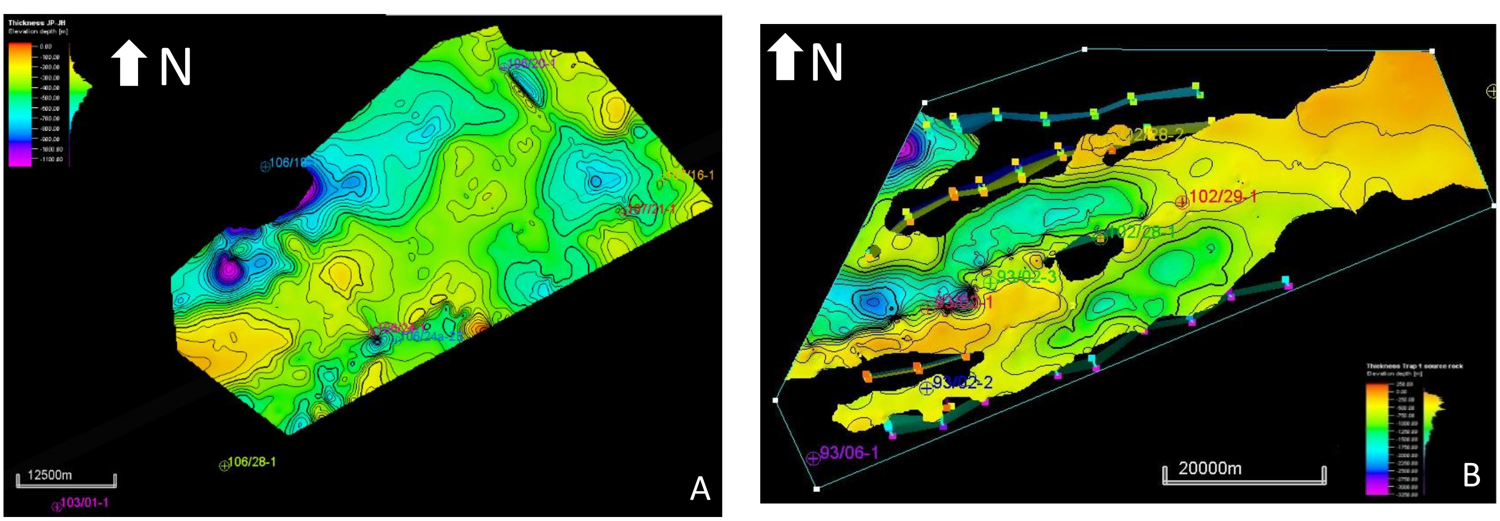

Figure 4.7: A: Thickness map SGCB of the source rock (from bottom Sinemurian to top Pliensbachian); B: Thickness map SCSB of the source rock (from bottom Hettangian to top Pliensbachian).

4.3 Burial history-1d Models (drilled wells)

The Fig. 4.8A shows the temperature for the well 106_18_1, the top of the source rocks, the Pliensbachian (JP), has a temperature greater than the 30°C, with a % Ro less than 0.5% and a Transformation Ratio (TR) of 0%. The sources rocks are immature, except for the bottom of the Sinemurian and the Hettangian which are at early maturity stages.

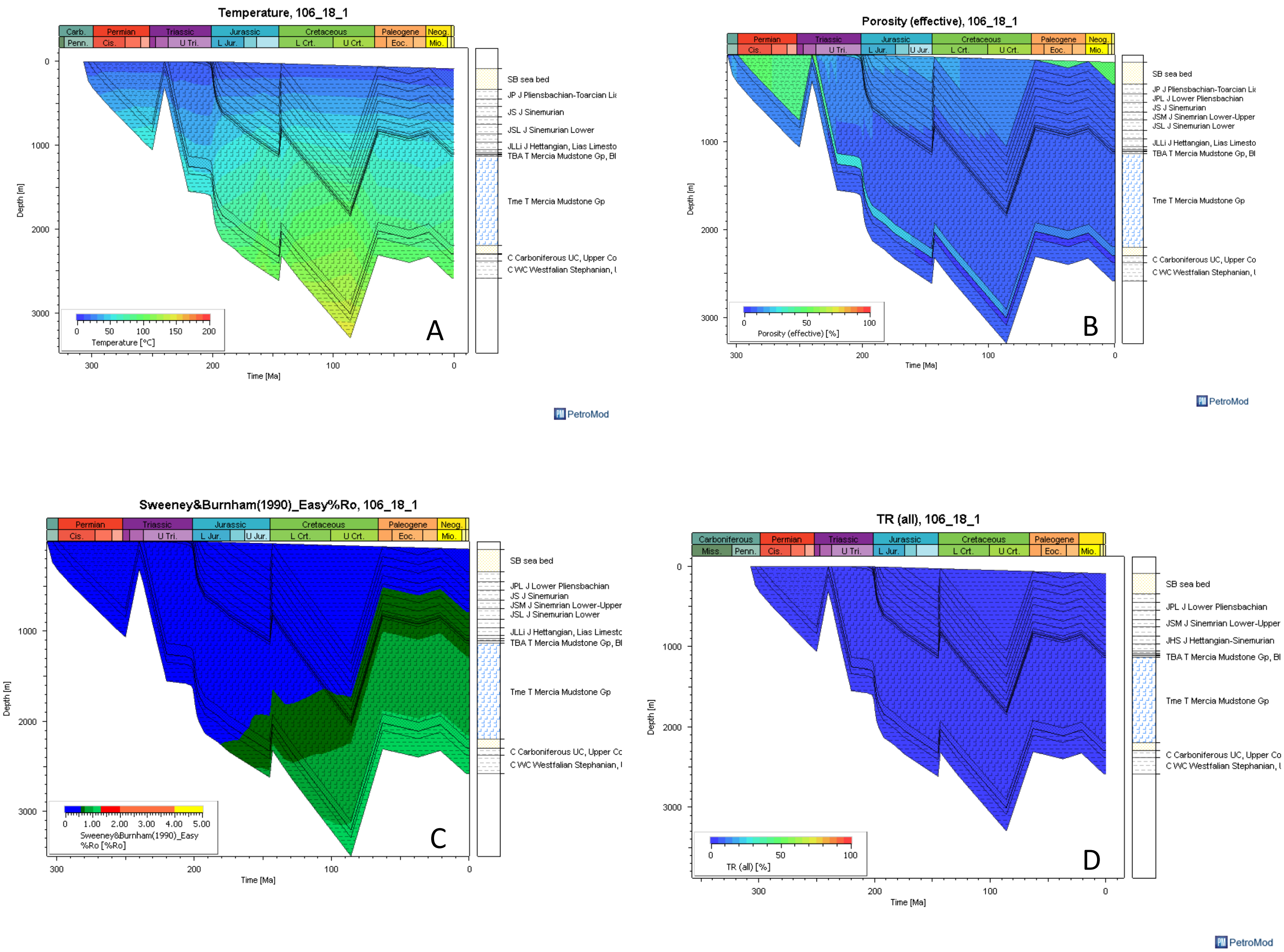

Figure 4.8: A: Burial plot/Temperature; B: Burial plot/Porosity; C: Burial plot/Ro; D: Burial plot/Transformation Ratio

The Table 4.4 shows the hydrocarbon generation potential, accumulation and expulsion for the rocks in this well. None of the units produced hydrocarbons, which is congruent with the classification of this well as dry (units are in MMBOE/km^2).

Table 4.4: Hydrocarbon generation potential, accumulation and expulsion well 106_18_1.

Source rock	Remaining potential	Generation Balance	Accumulated in source	Expelled HC
JP Pliensbachian-Toarcian Lias shale	11.95	0	0	0
J Lower Plienbachian	2	0	0	0
J Sinemurian	11.37	0	0	0
J Sinemurian Lower-Upper Lias Marl	1.99	0	0	0
J Sinemurian Lower-Upper Lias Marl	2	0	0	0
J Hettangian Sinemurian	1.23	0	0	0
J Hettangian, Lias Limestone	1.52	0.1	0	0.1
Total	**32.07**	**0.1**	**0**	**0.1**

In the well 103_1_1 there was a non-commercial gas discovery. The Fig. 4.9B shows that the Upper Jurassic has a Ro less than 0.5%. The Middle Jurassic has a Ro between 0.5 and 1.5% indicating maturity stages. In this well the Pliensbachian and Sinemurian are at an overmature stages. The temperature for the Pliensbachian is greater than 140°C (Fig. 4.9A). The Sinemurian has a TR of 83%.

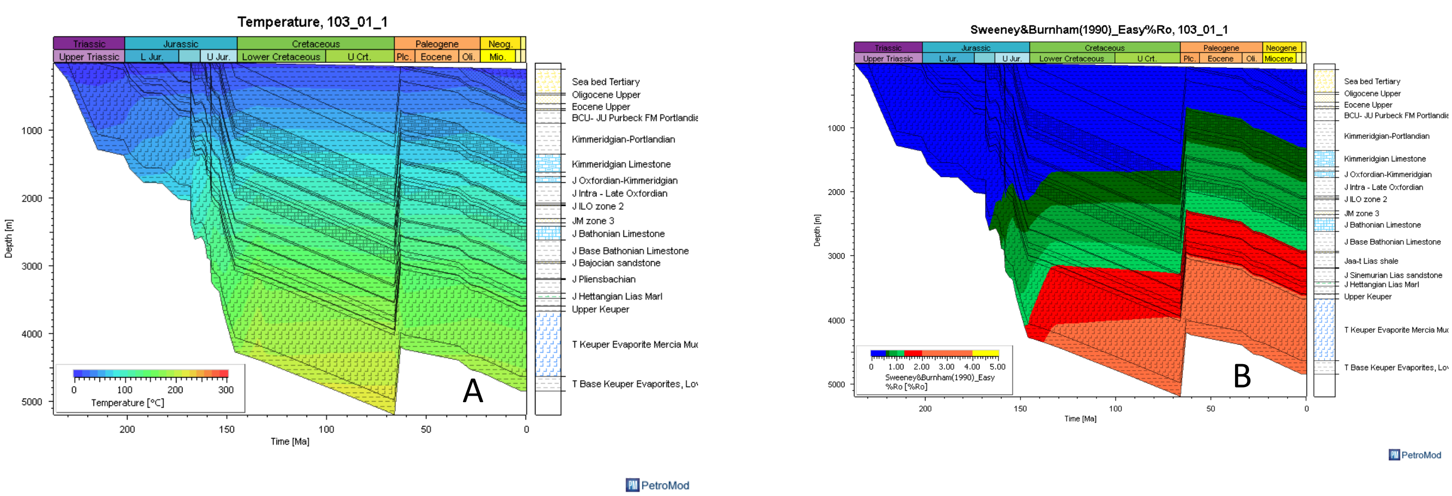

Figure 4.9: A: Burial plot/Temperature; B: Burial plot/Ro.

The Table 4.5 shows the hydrocarbon generation potential, accumulation and expulsion for the source rock in this well (units are in MMBOE/km^2).

Table 4.5: Hydrocarbon generation potential, accumulation and expulsion well 103_1_1.

Source rock	Remaining potential	Generation Balance	Accumulated in source	Expelled HC
Purbeck FM	8.49	0	0	0
Kimmeridgian-Portlandian	78.88	0.08	0.08	0
Kimmeridgian-Limestone	34.93	0.47	0.12	0.35
Kimmeridgian-Lower	21.21	0.92	0.05	0.86
J Oxfordian-Kimmeridgian	17.71	0.74	0	0.74
J Intra-Late Oxfordian	32.48	3.17	0.04	3.13
J Callovian-Middle Oxfordian	11.64	3.54	0	3.54
J Bathonian limestone	13.48	10.33	0.01	10.32
J Bajocian	0.14	0.32	0	0.31
Jaa-t Lias shale	1.05	2.83	0.06	2.78
J Sinemurian Lias	1.11	4.3	0.06	4.24
Total	**221.08**	**26.66**	**0.41**	**26.25**

4.6 Pseudo-wells characterization

4.6.1 Pseudo-wells characterization for the SGCB play

The Fig. 4.10A shows the time surface for the top of the Pliensbachian (provided by the seismic interpreter), the location of the target well and the pseudo wells. Four of the pseudo wells were located in the kitchen sector (Area 2.641658E+8 m^2) (PW-04, PW-05, PW-06 and PW-07) and three other wells near the trap (PW01, PW-02 and PW03). The Fig. 4.10B shows the NW-SE (AB) cross section that goes through the kitchen sector to the location of the trap.

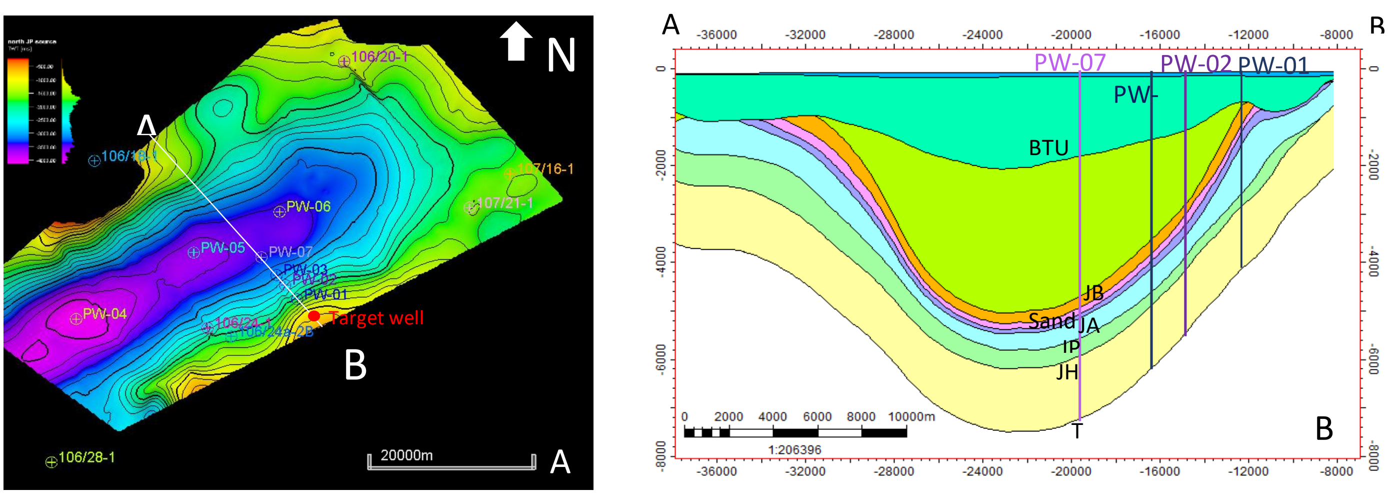

Figure 4.10: A: location of the pseudo wells; B: Cross section of the seismic depth model (provided by the seismic interpreter) near the trap with the pseudo wells.

Table 4.6 shows the total hydrocarbon generation at reservoir conditions (units are in MMBOE/km^2) for the pseudo well 01 and 04 with the P50, P90 and P10 (to see the parameters used for the probability cases, see Appendix 1.9). The PW-04 is the one with the highest amount of hydrocarbon generation with a total of 15.56 MMBOE/km^2 (P50), this is related to the geographical location of the well, which is located in the kitchen se1tor and the source rock is at 6,524 m. Meanwhile, the hydrocarbon generation is less for the PW-01 with a total of 13.34 MMBOE/km^2 (P50), where the Pliensbachian is at shallower depth (2687.03 m). In all wells, gas generation is higher than oil generation.

Table 4.6: Hydrocarbon generation pseudo wells 01 and 04 (units MMBOE/km^2).

PW/Source rock	P50		P90		P10	
	Vol. of oil	**Vol. of gas**	**Vol. of oil**	**Vol. of gas**	**Vol. of oil**	**Vol. of gas**
PW-01 JP	4.3	9.04	2.27	4.77	6.55	13.76
	P50		**P90**		**P10**	
	Vol. of oil	Vol. of gas	Vol. of oil	Vol. of gas	Vol. of oil	Vol. of gas
PW-04 JP	5.02	10.54	2.99	6.29	7.03	14.77

Table 4.7 shows that, by the Early Cretaceous 50% of the hydrocarbon was generated, with a volume of 6.67 MMBOE/km^2 for the PW-01, meanwhile for the PW-04, 50% the total volume of hydrocarbons was generated by Middle to Late Jurassic. The onset (5%) of the hydrocarbon generation and migration in the kitchen sector began at the end of the Middle Jurassic (approx. 167 MA, PW-04).

Table 4.7: Age at 5% and 50% of total generation for the pseudo wells 01 and 04 (P50).

PW	Source rock	Top Depth (m) (JP)	Bottom depth (m) (bottom JS)	Thickness (m)	Volume of hydrocarbon generated at 50%	Age at 50% HC generation (Ma)	Volume of hydrocarbon generated at 5%	Age at 5% HC generation (Ma)
PW-01	JP/JS	2687.03	2932.16	245.13	6.67	114.03	0.67	157
PW-04	JP/JS	6524.51	6709.82	185.31	23.66	163.35	2.37	167

The Fig. 4.11 shows the 2D model for the AB cross section (location at Fig. 4.10A) with maturity information. The main oil windows for the source rock start at 2,000 m and at depth of 2,800 m the rocks are in the wet gas window and in the deepest part the source rock is in overmature stages (below 5,700 m).

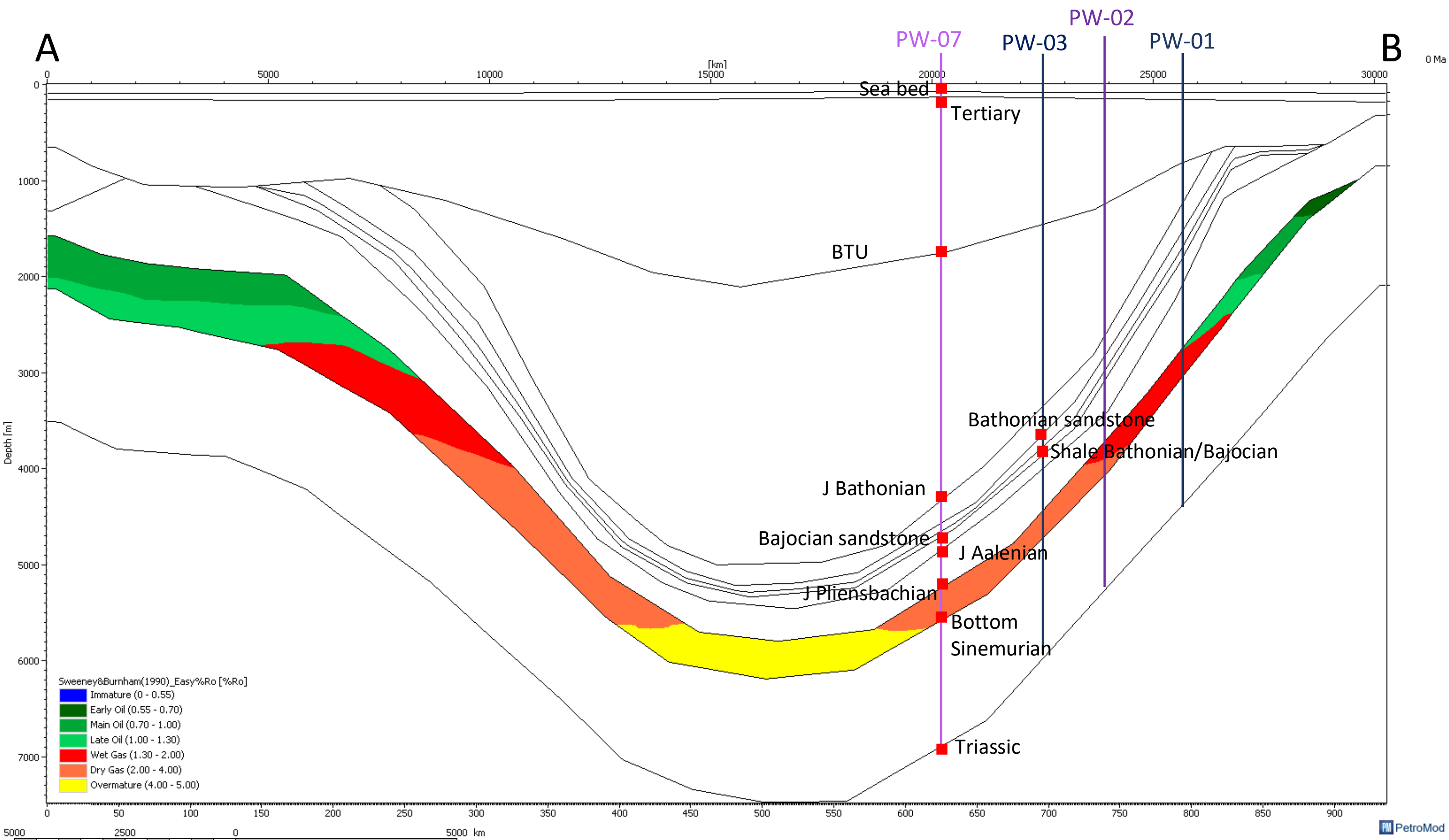

Figure 4.11: 2D model with maturity information for AB cross section.

4.6.2 Pseudo-wells characterization for the SCSB play

The Fig. 4.12 shows the depth surface for the top of the Pliensbachian (provided by the seismic interpreter) and the location of the pseudo wells, four of them are located in the kitchen sector (PW-08, PW-09, PW-10 and PW-11) and three others wells near the target trap (PW-12, PW-13 and PW-14). The kitchen sector has an area of 64579865 m^2.

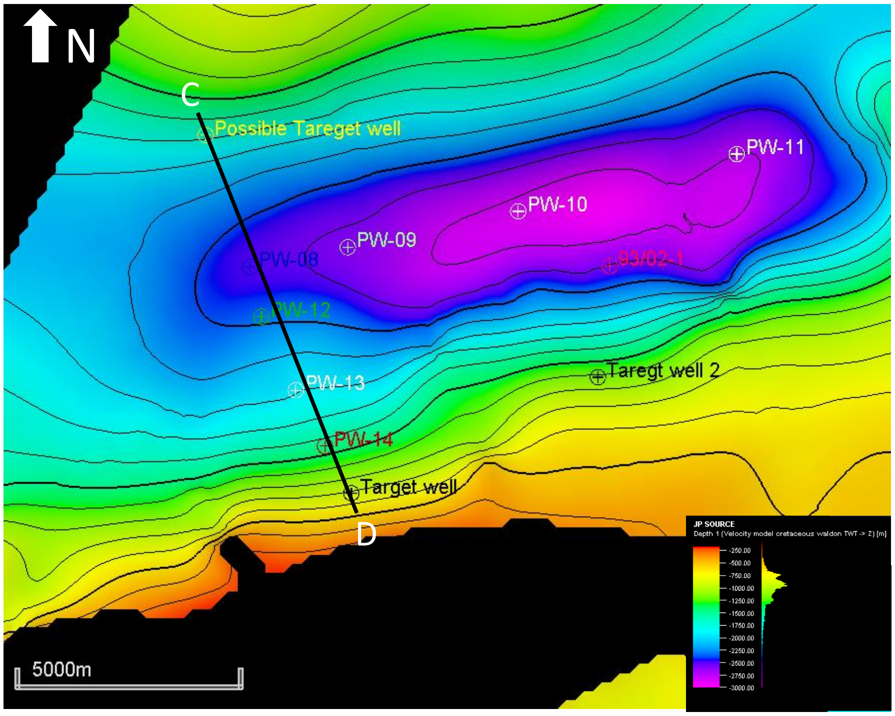

Figure 4.12: Location of pseudo wells. (Target well 2 is based on the seismic interpretation).

The table 4.8 shows the total hydrocarbon generation at reservoir conditions (units are in MMBOE/km^2) for the pseudo wells 08, 12 and 13 with the P50, P90 and P10. The PW-08 is located in the kitchen sector and the top of the source rock is at 2,605 m, this well has the highest amount of hydrocarbon generation with a total of 216.99 MMBOE/km^2 (P50), meanwhile the PW-14 has a total generation of 0.09 MMBOE/km^2 (P50), this low value is related to immature to early maturity stages (Fig. 4.13) of the source rock (top of the Pliensbachian at 1,461 m).

Table 4.8: Hydrocarbon generation pseudo wells 08, 12, 13 and 14 (units MMBOE/km2).

PW/Source rock	P50		P90		P10	
	Vol. of oil	Vol. of gas	Vol. of oil	Vol. of gas	Vol. of oil	Vol. of gas
PW-08 JP-JH	69.99	147	40.21	84.49	101.14	212.52
	P50		**P90**		**P10**	
	Vol. of oil	Vol. of gas	Vol. of oil	Vol. of gas	Vol. of oil	Vol. of gas
PW-12 JP-JH	48.03	100.92	27.25	57.27	70.89	148.96

	P50		P90		P10	
	Vol. of oil	Vol. of gas	Vol. of oil	Vol. of gas	Vol. of oil	Vol. of gas
PW-13 JP-JH	6.71	14.11	3.07	6.45	11.81	24.81
	P50		**P90**		**P10**	
	Vol. of oil	Vol. of gas	Vol. of oil	Vol. of gas	Vol. of oil	Vol. of gas
PW-14 JP-JH	0.03	0.06	0.02	0.01	0.07	0.14

Table 4.9 shows that by the Late Jurassic 50% of the hydrocarbons were generated and the onset of the hydrocarbon generation (5%) started in the Toarcian (P50 PW-09 located in the kitchen sector). For this play, the source rock was formed in the Lower Jurassic, the reservoir (sandstone, Wealden Formation) was formed in the Albian and the seal unit in the Cenomanian (shale from the Gault Equivalent). As mentioned before, the generation and expulsion started in the Early/Middle (PW-09) to Upper Jurassic (PW-13) and at that time the reservoir and seal units were not formed, after the seal unit was formed (after 100 MA), 16% of the total volume of hydrocarbons (37 MMBOE/km^2, P50) were still to be generated for the PW-09.

Table 4. 9: Age at 5% and 50% of total generation for the pseudo wells 09 and 13 (P50).

PW/Source rock	Top Depth (m)	Bottom depth (m)	Total volume of HC generated	% HC generated at 100 MA	Volume of HC generated at 100 MA	Volume of expulsion at 100 MA	Age at 5% HC generation (Ma)	Age at 50 % HC generation
PW-09-P50	2604.71	4966.29	217.06	84	183	181	180	162
PW-13-P50	1915.97	2825.07	20.82	48	10.13	9.4	160	94

Table 4.10 shows the total volume and the volume of hydrocarbons that the source rock will generate after the formation of the seal unit (after 100 MA). The percentage that will generate goes from 15 (PW-12) to 50 % (PW-13) of the total volume. There is no expulsion in the PW-14 because there is not enough hydrocarbon generation.

Table 4.10: Total Hydrocarbon generation per pseudo wells and considering the remnant generation after the seal was formed.

PW/Source rock	Total volume of HC generated	Vol. generated at 100 MA	% generated at 100 MA	Volume of expulsion at 100 MA	Volume Hydrocarbons still to generate after 100 MA
PW-08 JP P50	**217.07**	183.16	84.38	181.37	**33.91**
PW-08 JP P10	**313.66**	269.21	85.83	267.47	**44.45**
PW-08 JP P90	**124.7**	103.57	83.06	101.73	**21.13**
PW-12 JP P50	**148.94**	132.19	88.75	130.74	**16.75**
PW-12 JP P10	**219.85**	198.41	90.25	197.38	**21.44**
PW-12 JP P90	**84.53**	72.51	85.78	71.07	**12.02**
PW-13 JP P50	**20.82**	10.13	48.65	9.46	**10.69**
PW-13 JP P10	**36.62**	18.64	50.89	17.98	**17.98**
PW-13 JP P90	**9.52**	4.38	45.99	3.59	**5.14**
PW-14 JP P50	**0.09**	0.07	73.7	0	**0.02**
PW-14 JP P10	**0.21**	0.16	76.26	0	**0.05**
PW-14 JP P90	**0.03**	0.02	71.13	0	**0.01**

The Fig. 4.13 shows the 2D model with maturity information, the main oil windows for the source rock started at an approximate depth of 1,800 m, at depth of 3,500 m the rocks are in the wet gas window and in the deepest part the source rock is at dry gas stages (below 4,300 m).

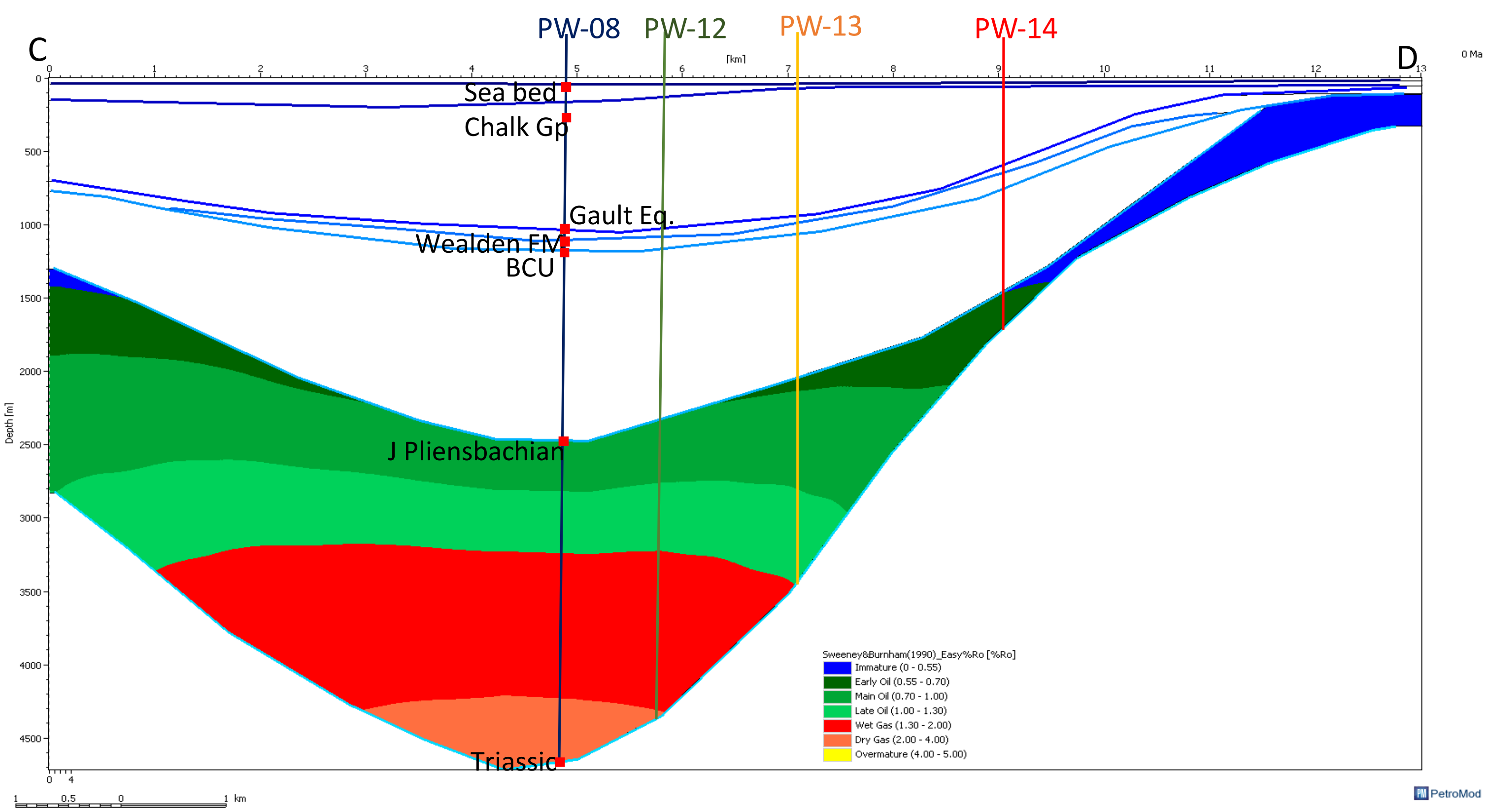

Figure 4.13: 2D model with maturity information for CD cross section (location in Fig. 4.12).

5. Discussion

The analyzed kerogen composition indicates a terrestrial input which could be related to the proximity of the basin to the coast, this could explain the high scattering in the kerogen composition. Moreover, the TOC content is higher for the SCSB compared with the SGCB, this could be related also to the distance of the coast, as the marine inversion occurred from the SE to the NW, and because of that, the SGCB is the one that was nearer the coasts, yielding a spatial variations of TOC at a regional scale. Moreover, according to seismic and literature, the Pembrokeshire Ridge (Shannon, 1995; Shannon & Naylor 1998) is located between the SCSB and the SGCB, there was a discontinues topographic high that was formed in the Triassic, that could have affected the preservation of the organic matter in the SGCB.

The present day average geothermal gradient calculated for SCSB prospect (Appendix 1.10) is 51.3°C/km and for the NCSB is 44°C/km, this high value could be due to lack of measurements (only 10 wells have data with no more than 3 data points) or an error caused by bad quality data (most of the well do not have circulation time, and the Borehole Temperature Correction was done adding 18°C/km, 'Last Resort Correction' ZetaWare website). According to Corry & Colin (1998), the average for the geothermal gradient for the Celtic Sea Basin is 32°C, with a range from 21°C/km for Wealden and 53°C/km and 42°C/km for the Quaternary and Chalk respectively. Moreover, near the SCSB there are three major granites batholiths intruded in the Early Permian into Devonian-Carboniferous units, called Haig Fras Batholith with a total length of 46 km and a width of 14 km. These batholites are at distance from the SCSB of 15 km to the SW (gravimetric map with batholiths, Appendix 1.11), and the remnant heat and heating by radioactive decay in granite could affect the geothermal gradient in the sector.

The source rock in most of the drilled wells are thermally immature because the source rock is not deep enough to generate hydrocarbons at the drilling site. In the SCSB, only two wells are immature to early mature: the 93_02_3 (SCSB) which has traces of gas, and the Pliensbachian source rock has a Ro of 0.55% at 1,500 m. The other early mature well in the SCSB is the 93_2_1 (Appendix for 1.2, figure 1.2.2), in which the Middle Jurassic strata has a Ro of 0.7% (mature after 1,500 m). In the SGSB, the source rock (Lower Jurassic) of the well 103_1_1 (non-commercial gas discovery) is overmature (Ro of 0.8%) and it is a depth greater of 3,100 m.

The main unconformity that is related to the erosion of the Jurassic rocks in the Celtic Sea basins, is the Late Jurassic to Early Cretaceous unconformity (BCU). The amount of Upper and Middle Jurassic strata that was eroded from the BCU is greatest in the South-West (SCSB play) where none of the wells intercepted the Upper Jurassic and the stratigraphy goes from Lower Jurassic (in most of the cases or in some Middle) to Early Cretaceous, and decreases to the North-East (SGCB play) where Upper Jurassic was found in some wells. The other important maturity control is the Cenozoic Unconformity (BTU), one of the conclusions from the stratigraphy of the wells is that the BTU eroded greatest amount of cretaceous strata in the North-East part (SGCB play). It's probable that some amount of erosion from the BCU has been overprinted by the later BTU, in this scenario the BTU overprinted the early unconformity leading to the Late Jurassic being eroded. According to the thermal maturity of the drilled wells, most of them are immature which could be related to the erosion episodes where the cessation of burial caused by the uplift followed by the erosions events stopped the thermal maturity of the source rock. The Jurassic source rock distribution will be related to the presence or absence and the amount of the BCU. In the well 103_1_1 where there is a complete Jurassic stratigraphy and the source rock was found to be overmature, at present time. Besides, in the well 93_2_3, the Middle Jurassic was not eroded by the BCU, and the lower Jurassic source rock was found to be early mature.

The 1D model for the drilled wells shows a good to fair remaining potential, with a very low transformation ratio for all wells. Only the well 103_1_1, shows a TR up to 83%, this high value suggests that the oil that was generated was cracked into gas, in this well a non-commercial gas discovery was found, and the source rock is believed to be from the Lower Jurassic which at present time is overmature, all others potential rocks are immature.

The 1D model for the pseudo wells shows that the source rock reached the maturity stages, for the SCSB play below 1,500-2,000 m and for the SCGB below 1,800-2,000 m, and in the deepest zone the source rock is overmature, this can be seen in the 2D model as well, the drilled wells weren't located in kitchen sectors thus the source rock is not deep enough to generate hydrocarbons.

6. Appraising new prospect on the basis of your assignment

For the SCSB, the 2D model with the migration vectors and hydrocarbon accumulation is shown in Fig. 4.14 , the deepest faults are acting as a migration pathway from the source rocks to the reservoir unit. There are two possible hydrocarbon accumulations, both are located above the oil-water contact (1,100 m according to the seismic interpreter), therefore two possible targets are proposed. The accumulation in the NW sector is located at 882 m, and the one in the SE is at 222 m. The 2D model calculates the potential amount of hydrocarbon generation and the software does not consider the timing of the seal formation, therefore the hydrocarbon that was generated before the seal formation is lost and the accumulation volumes that PetroMod gives need to be corrected, considering only the generation after 100 MA (after the seal unit was formed). According to the pseudo wells analysis, the hydrocarbon that will generate after the seal was formed goes from 15 (PW-12) to 50 % (PW-13) of the total volume, therefore an approximate number of 20 % of the total volume is considered (Table 4.11).

Table 4.11: Total hydrocarbon accumulation in the prospect at reservoir conditions and possible accumulation after the seal was formed.

Accumulation NW		
Hydrocarbon	Total volume accumulated	Possible volume accumulated after 100 million years (after Gault formation)
Oil (MMbls)	960	192
Gas (Mm³)	20412.38	4082.476

Accumulation SE		
Hydrocarbon	Total volume accumulated	Possible volume accumulated after 100 million years (after Gault formation)
Oil (MMbls)	1778.22	355.644
Gas (Mm³)	42043.07	8408.614

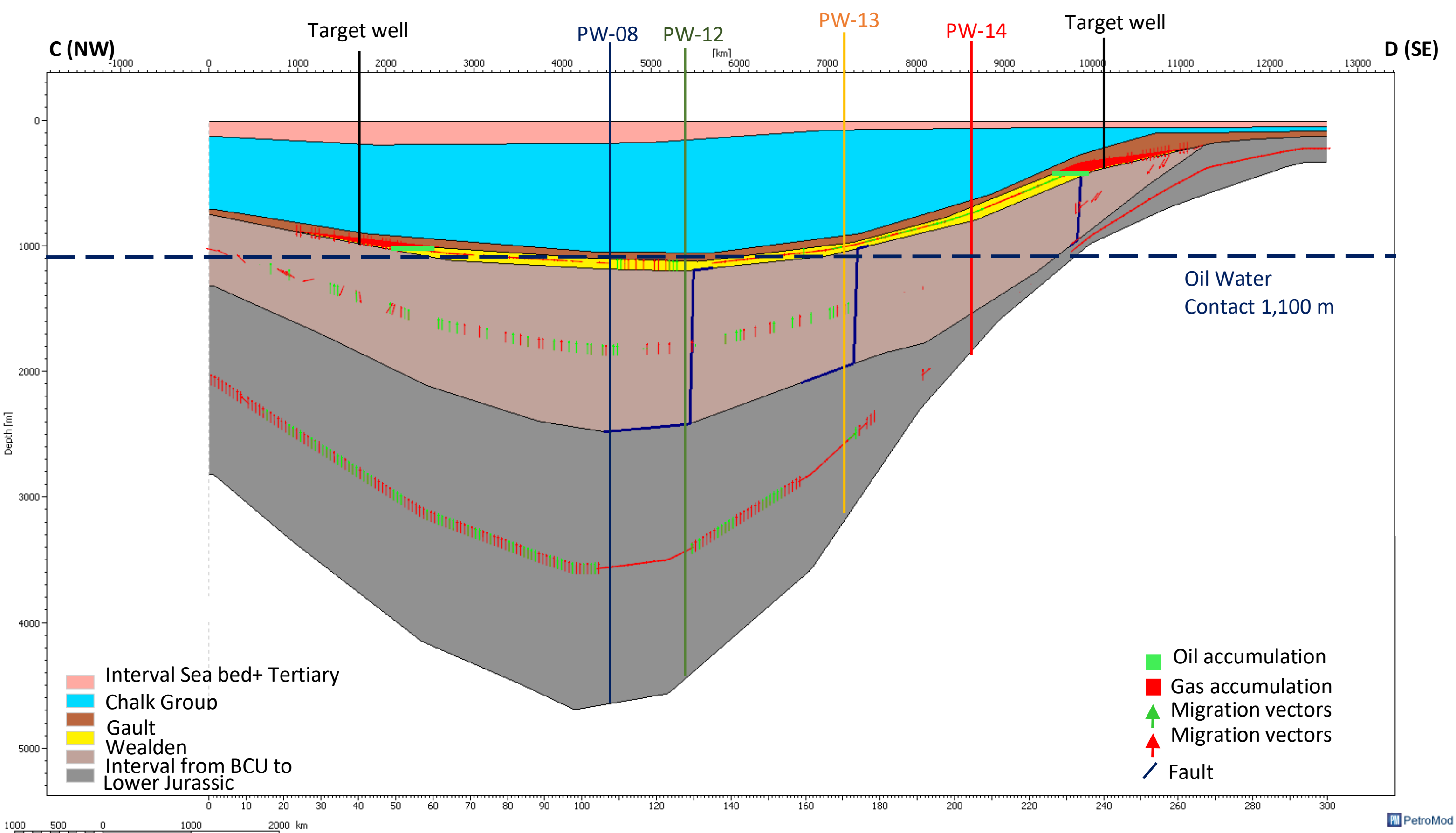

Figure 4.14: 2D model for the CD cross section (location at Fig 4.12).

For the SGCB, the 2D model with the migration vectors and hydrocarbon accumulations are shown in Fig 4.15 (vertical and lateral migration were considered in the software), the deepest faults are acting as a migration pathway from the source rocks to the reservoir unit. According to the 2D model, there are two possible accumulation of hydrocarbons, one is located in the NW of the cross section at 1,053 m and the other is in the SE part, at 716 m. Considering that the oil water contact is at 1,328 m (according to the seismic interpreter), both accumulation could be considered as possible targets, but where the NW accumulation is located there is not a four-way closure (no closure in NE direction), therefore only one target well is proposed, where the SE accumulations is.

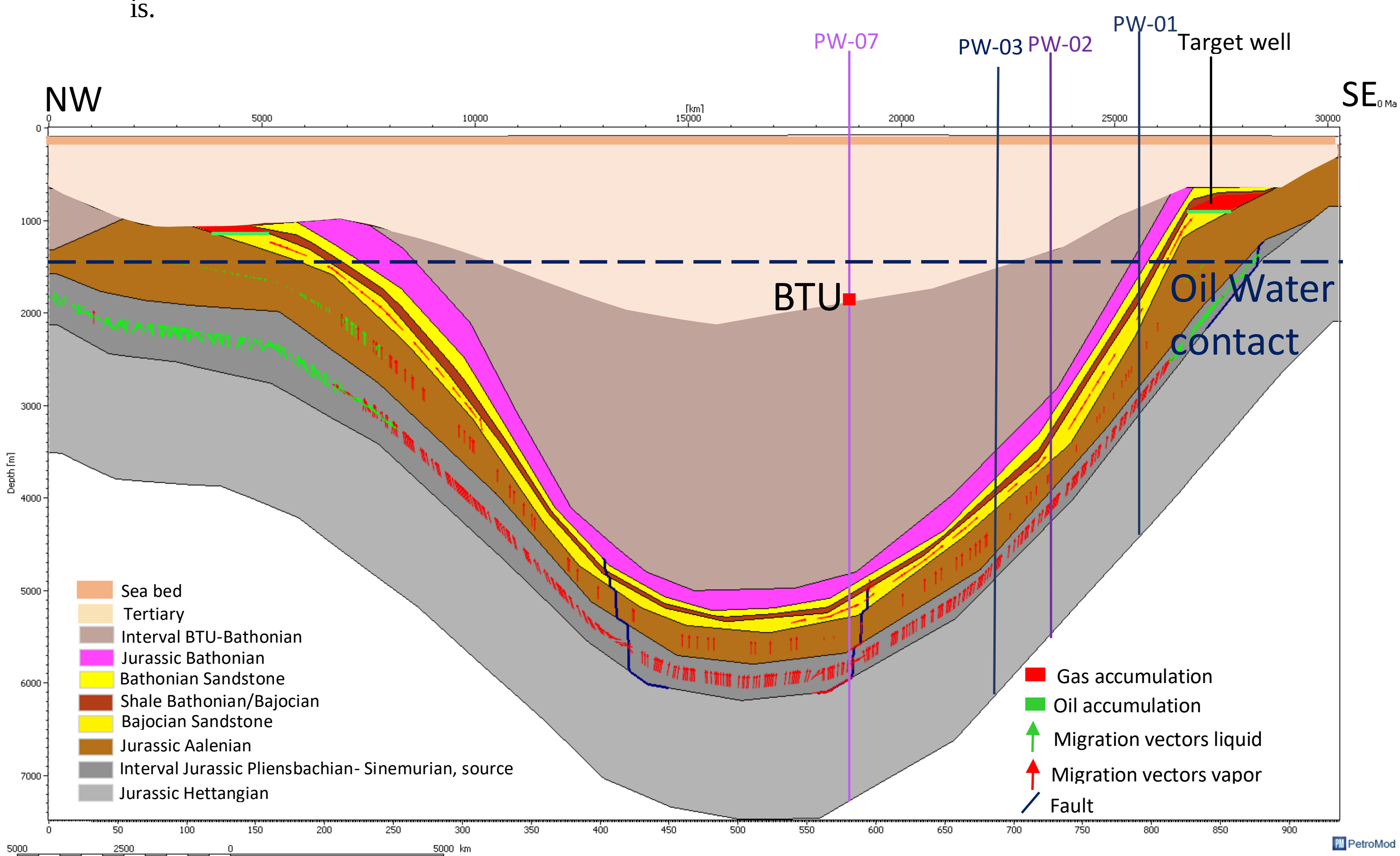

Figure 4.15: 2D model for the AB cross section (location at Fig 4.10A).

Table 4.12 shows the Hydrocarbon accumulation at reservoir conditions where the target well is proposed (SE) (PetroMod assumes the section maintains its geometry to a distance of 500m either side of the accumulation, therefore the total width considered for the accumulation is 1km) and the accumulation in the NW where a trap was not found. Both values are congruent with the 1D hydrocarbon generation of the pseudo wells.

Table 4.12. Hydrocarbon accumulation.

Accumulation target well (SE)	
Oil (MMbbls)	3.15
Gas (Mm^3)	39555.7

Accumulation in the NW	
Oil (MMbbls)	28.51
Gas (Mm^3)	25487.27

7. Assessment of risk-uncertainties and probability of geological success (source rock)

The major risk is related to the lack of data, such as pore pressure tests (being the only data available the mud weight), porosity, permeability, among others. There is not enough data of BHT, with some data being anomaly high for this tectonic setting. There is an uncertainty in the calibration which is related to possible errors in the calibrated wells, for instance the vitrinite, temperature data does not have error bars. One major uncertainty is the kinetic model used for the hydrocarbon generation, due to a lack of studies of kinetic models in the basin, the Burnham *et al.*, (1989) global kinetic model was used.

Another important risk is related to lack of consistency in the stratigraphy, there is not a formal lithostratigraphy in this sector, which makes a unified lithological characterization hard.

Another risk is related to a possible hydrocarbon alteration, that could change the chemical properties of the hydrocarbons in the trap, such as biodegradation.

According to the geochemical characterization of the source rock, the probability of success is 0.75, for both studied sectors. For the thermal maturity of the source, there is a success of 0.75

studied sectors, the source will be thermally mature in depocenters, according to the 2D model for the SCSB prospect, the source rock is at the main oil window below 1,800 m, meanwhile in the SGSB is found below 2,000 m. At shallow depth the rocks will be immature. For the accumulations, must be taken into account the timing of the petroleum system, which is discussed in Chapter VI, for instance, for the SCSB sector not all the hydrocarbons generated will be able to accumulate in the reservoir unit, because the reservoir and seal were formed after the generation started. Therefore, the timing success for both plays will be different, there will be more success for the SGSB, 0.85 (where there is a favorable petroleum system timing), than for the SCSB (0.65).

8. Source rocks analogs

There are several fields where the hydrocarbon was generated from the Lower Jurassic rocks. The Ballycotton gas field was discovered in 1989 (Croker & Shannon, 1995). The Lower Jurassic, which was formed by a transgression, is believed to be the major source rock in this region.

The Brandon discovery in the Slyne Basin (Ireland), is a gas field from Lower Jurassic source rocks, the Pliensbachian interval has a TOC of 5% and HI of 400 mg HC/g TOC (Carlisle, 2017).

The Dragon Discovery (drilled by Marathon Oil Plc in 1994 to test the Jurassic "Dragon" prospect, well 103_1_1) is located in the boundaries of Ireland and the UK, in the St George's Channel. Corresponding to a gas Discovery in sandstone reservoirs of the Middle Jurassic age, the gas was trapped in the footwall of a normal fault. The source rock is believed to be from the Lower Jurassic. The resources of gas were not commercial (at most of 51 bcf of gas according to the Marathon Oil, Relinquishment Report Block 103/01a). Later in 2005, well 103/01a-2 was drilled to test the continuity of the gas within the sandstone across a fault block near the well 103/1-1, but the well was dry hole in the same equivalent-aged sandstones. This hydrocarbon has 46° API cond.

(Scotchman, 2001). Even though this discovery is not commercial it is important because it's the only one located in the study area.

Another field where the source rock was from the Lower Jurassic is the Helvick with an accumulation of 2-5 MMBO, with a 44° API oil and 58° for the condensate, was found in Middle-Upper Jurassic sandstone (Caston, 1995).

9. Conclusions

The conclusion of the geochemical characterization of 12 drilled wells, was the Lower Jurassic (from Hettangian to the Pliensbachian) a main source rock at a regional scale, due to the highest mean value and a homogenous population. For the SCSB, the Sinemurian is the interval with higher TOC content with 2.47% followed by the Pliensbachian with 1.58 % and the Hettangian with an average of 1.5%. On the other hand, in the SGCB the Pliensbachian interval is the one with higher TOC content (1.49%) followed by the Sinemurian with 1.24 %, the Hettangian is not considered in this basins, as a potential source rock due to the TOC content (0.8%). It can be seen a spatial distribution of TOC content, being high in the SCSB which could be related to the distance of the coast and the direction of the marine transgression (to the NW). The source rocks in both basins have a good thickness and a good lateral continuity.

There is a good hydrocarbon generation potential for the Lower Jurassic, according to the 1D model of the drilled wells. According to the pseudo wells, the SGSB has less amount of hydrocarbon generation (compared with the SGCB), this is related to a less TOC value and a less thickness of the source rock (400 m average).

The transect of the 2D model was through the kitchen sector to the trap locations. For the SGSB prospect, the source rock is at the main oil window below 2,000 m, and according to the 2D model and the analysis of the trap, there is one possible accumulation of hydrocarbon located at 716 m, where one target well is proposed, with oil accumulations of 3.15 MMbbls and gas accumulation of 39555.7 Mm^3.

Meanwhile the source rock in the SCSB is mature below 1,800 m, and is immature at shallower depths. There are two possible hydrocarbon accumulations, one in the NW part and other in the SE part of the cross section, where two target wells are proposed. The NW accumulation has a possible accumulation of 192 MMbls of oil and 4082.476 Mm^3 of gas, meanwhile, the one at the SE, has 355 MMbls of oil and 8408.614 of gas.

The BCU is one important control in the preservation and maturity of the Lower Jurassic source rocks.

10. Suggestion of further work

In order to have a better geochemical characterization, HI, TOC and vitrine reflectance is need in more wells from the Lower Jurassic. In future wells a pressure measurement can be done, that will improve the calibration process. A regional kinetic model for the Celtic Sea basin with emphasis in the Lower Jurassic source rock can be done, that will improve the calculation of the hydrocarbon generation of the pseudo wells and the accumulation in the 2D model.

11. References

Carlis, M. (2017). Geochemical study of hydrocarbonprone sediments of Lower Jurassic age in the Slyne Basin, offshore Ireland.

Caston, V. (1993). The Helvick oil accumulation, Block 49/9, North Celtic Sea Basin. Geological Society, London, Special Publications.

Corry, D & Brown, C. (1998). Temperature and heat flow in the Celtic Sea basins. Petroleum Geoscience.

Croker, F & Shannon, M. (1995). The petroleum geology of Ireland's offshore basins: introduction. In P. F. Croker & P. M. Shannon, eds. The Petroleum Geology of Irelands Offshore Basins, Geological Society Special Publication. pp. 101–137.

Hillis, R. (1988). The Geology and Tectonic Evolution of the Western Approaches Trough. University of Edinburgh.

Lee, J. (2017). The Jurassic Source Rock Potential of the Celtic Sea and Western Approaches. Master Thesis, Durham University.

Marathon Oil, Licence P804 , Block 103 / 01a ALL , Relinquishment Report. , pp.1–5.

McElwain, D.J. Beerling and F.I. (1999). Fossil plants and global warming at the Triassic–Jurassic boundary J. Woodward Science.

McMahon, N.A & Turner, J. (1998). The documentation of a latest Jurassic-earliest Cretaceous uplift throughout southern England and adjacent offshore areas. In: Underhill, J. R., ed. Development, Evolution and Petroleum Geology of the Wessex Basin, Geological Society, London, Special Publications, 133, pp.215-240.

Rowell, P. (1995). Tectono-stratigraphy of the North Celtic Sea Basin. Geological Society, London, Special Publications, 93(1), 101–137. https://doi.org/10.1144/GSL.SP.1995.093.01.11

Ruhl, M; Hesselbo, S; Hinnov, L; Jenkyns, H; Xu, W; Riding, J; Storm, M; Minisini, D; Ullmann, C; Leng, M. (2016). Astronomical constraints on the duration of the Early Jurassic Pliensbachian Stage and global climatic fluctuations. Earth and Planetary Science Letters, 1, pp.1–17. Available at: http://dx.doi.org/10.1016/j.epsl.2016.08.038.

Scotchman, I. (2001). Petroleum geochemistry of the Lower and Middle Jurassic in Atlantic margin basins of Ireland and the UK. In P. M. Shannon, P. D. W. Haughton, & D. V Corcoran, eds. The Petroleum Exploration of Ireland's Offshore Basins. Geological Society, London, Special Publications, 188. pp. 31–60.

Shannon, P & Naylor, D. (1998). An assessment of Irish offshore basins and petroleum plays. Jpurnal of Petroleum Geology, vol 21(2).

Shannon, P. M. (1995). Permo-Triassic development of the Celtic Sea region, offshore Ireland. Geological Society, London, Special Publications, 91(1), 215–237. https://doi.org/10.1144/GSL.SP.1995.091.01.11.

Tugend, J. (2014). Formation and deformation of hyperextended rift systems: Insights from rift domain mapping in the Bay of Biscay-Pyrenees. Tectonics, 33, pp.1239–1276.

12. Acknowledgments

This study contains information provided by the Oil and Gas Authority and/or other third parties. Thanks to Schulmberger for the license donation of Petrel, Techlog and PetroMod used in this study. Thanks to Professor Dr. Elena Konstantinovskaya, Dr. Nicholas Harris, PhD Martin Schwangler, PhD Rafael Becerra Delmoral and PhD Noga Vaisblat for technical and geological support.

Thanks to ANII for the financial support and MIEM. Thanks to my friends and colleagues of Hidrocarburos-MIEM. Thanks to all my professor at the Universidad de la República and University of Alberta for helping me understand from the beginning what geology and science are about.

A big thanks to Carlo Azuara, Ana Ortega and Martín Gepp and to all my friends around the world. Thanks to my lovely family **-ALELILUNAMAR-** for being always there.